Electronic Supplementary Material (ESI) for Journal of Materials Chemistry A.

Supplementary Information

Facile synthesis of porous MgO-CaO-SnO_x nanocubes implanted firmly on in-situ formed carbon paper and their lithium storage properties

Bote Zhao,[ab] Guangming Yang,[ab] Ran Ran,[ab] Chan Kwak,*[c] Doh Won Jung,[c] Hee Jung Park[c] and Zongping Shao*[ad]

[a] State Key Laboratory of Materials-Oriented Chemical Engineering, Nanjing University of Technology, Nanjing 210009, China.

[b] College of Chemistry & Chemical Engineering, Nanjing University of Technology, Nanjing 210009, China

[c] Samsung Advanced Institute of Technology (SAIT), 14-1 Nongseo-dong, Yongin-si, Gyunggi-do, Korea 446-712.

[d] College of Energy, Nanjing University of Technology, Nanjing 210009, China

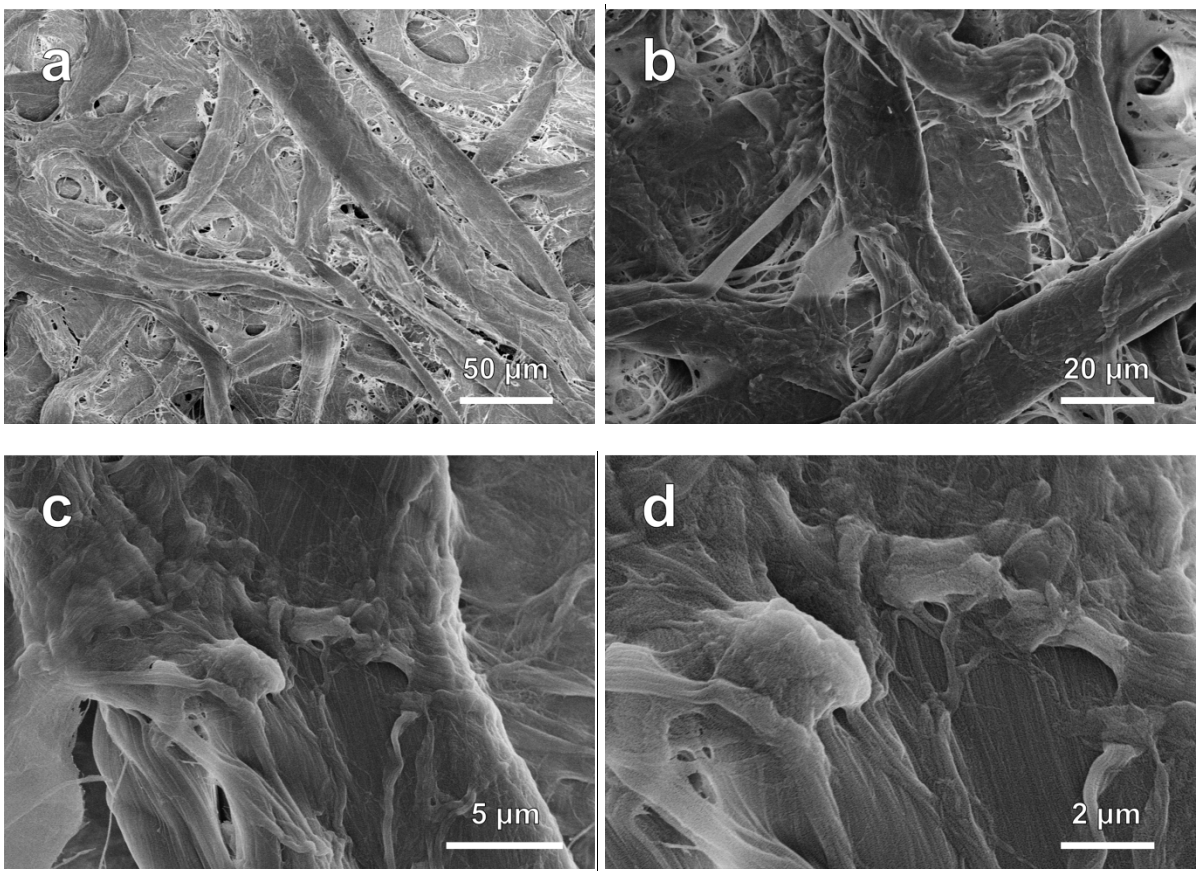

Figure S1. (a-d) FE-SEM images of acid activated filter paper.

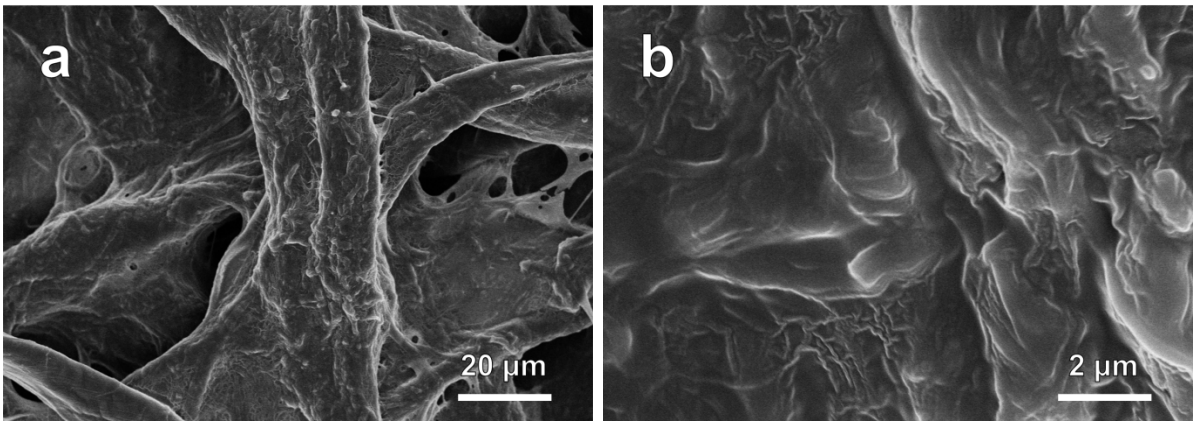

Figure S2. (a, b) FE-SEM images of filter paper after adsorption of tin(II) octanoate.

Figure S3. Digital photo of precursor cubes/filter paper by treating the absorbed composite paper in boiling Mg^{2+}/Ca^{2+}-containing water (300 mL) with 1 mL of $NH_3 \cdot H_2O$ for 1 h.

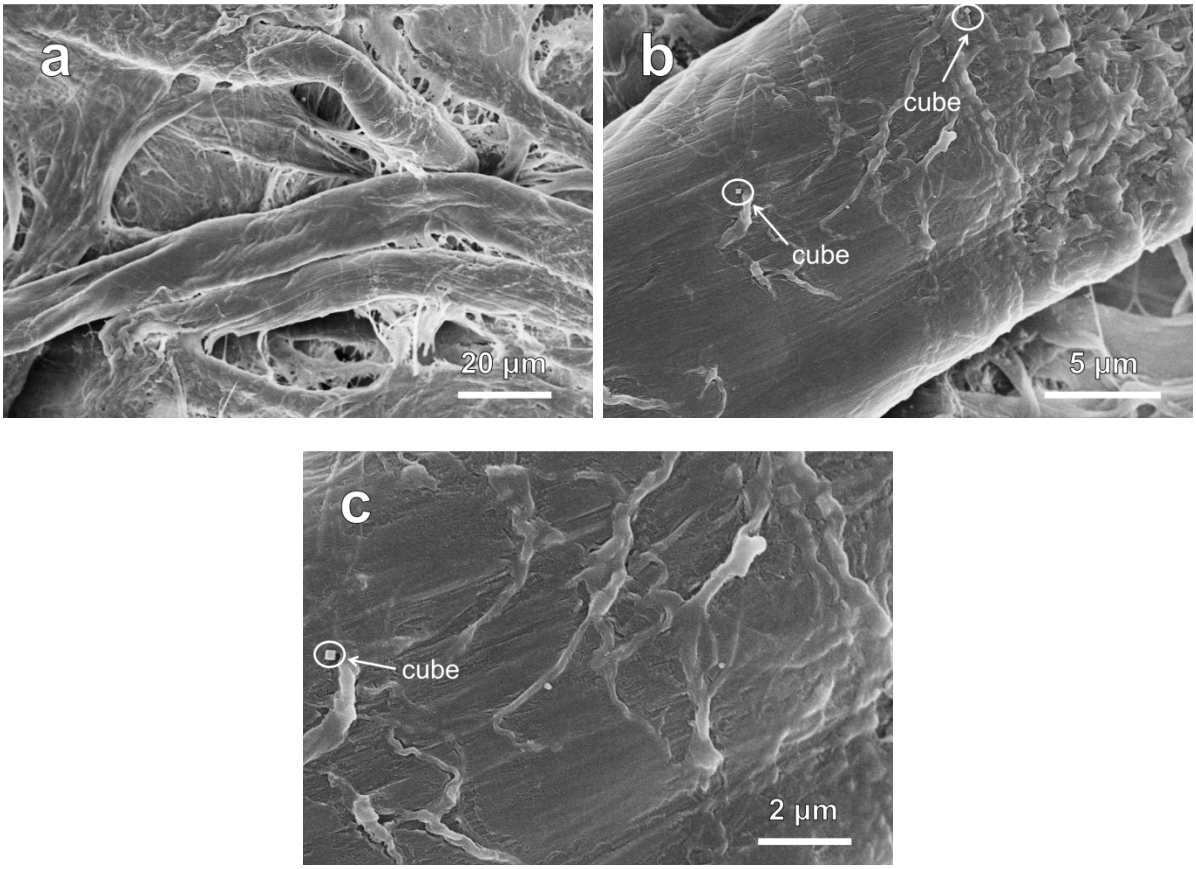

Figure S4. (a-c) FE-SEM images of composite paper after treating the absorbed composite paper in boiling deionized water (300 mL) with 1 mL of $NH_3 \cdot H_2O$ for 1 h.

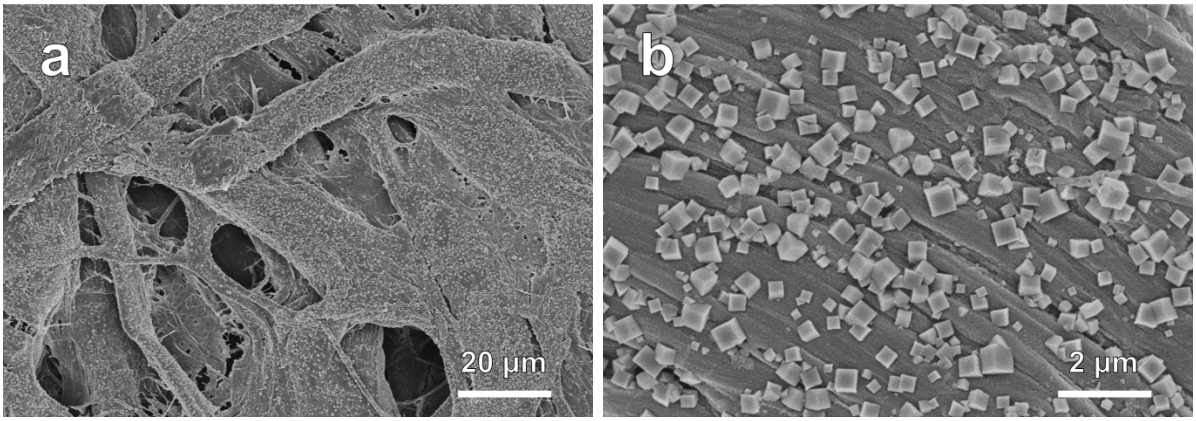

Figure S5. (a, b) FE-SEM images of composite paper after treating the absorbed composite paper in boiling Mg^{2+}-containing water (7.7 mg L^{-1}, 300 mL) with 1 mL of $NH_3 \cdot H_2O$ for 1 h.

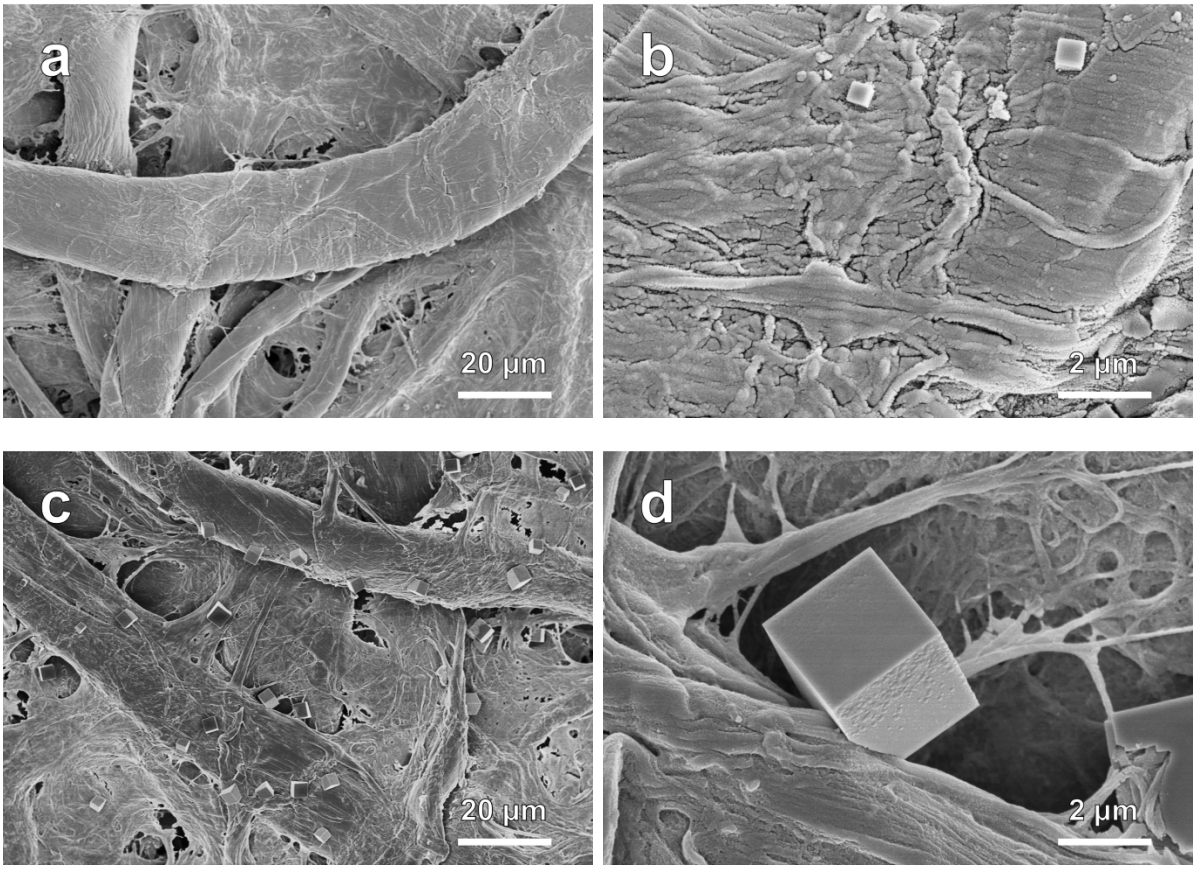

Figure S6. FE-SEM images of composite papers after treating the absorbed composite papers in boiling Ca^{2+}-containing water (300 mL) with 1 mL of $NH_3 \cdot H_2O$ for 1 h with Ca^{2+} concentration of (a, b) 12.7 mg L^{-1} (0.095 mmol) and (c, d) 39.6 mg L^{-1} (0.296 mmol).

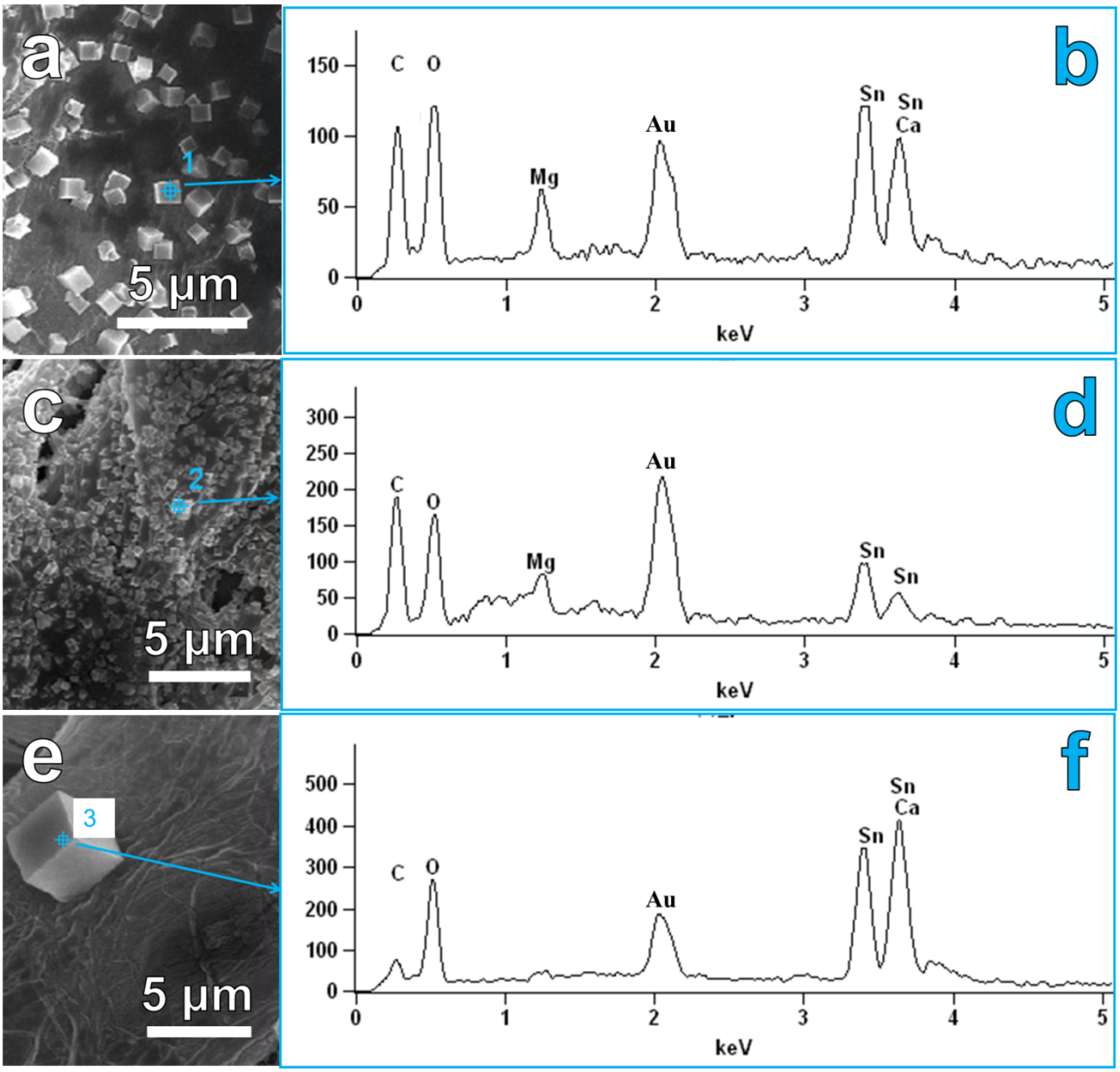

Figure S7. FE-SEM images of composite papers after treating the absorbed composite papers in boiling (a) Mg^{2+}/Ca^{2+}-containing water (300 mL, 7.7 mg L^{-1} of Mg^{2+} and 39.6 mg L^{-1} of Ca^{2+}) with 1 mL of $NH_3 \cdot H_2O$ for 1 h, (c) Mg^{2+}-containing water (300 mL, 7.7 mg L^{-1} of Mg^{2+}) with 1 mL of $NH_3 \cdot H_2O$ for 1 h, (e) Ca^{2+}-containing water (300 mL, 39.6 mg L^{-1} of Ca^{2+}) with 1 mL of $NH_3 \cdot H_2O$ for 1 h; (b, d, f) EDX spectra from "1", "2", "3" sites in Figure S7a, Figure S7c, Figure S7e, respectively. The signal of Au is generated from the surface coating by sputtering to minimize charging effects under FE-SEM imaging conditions.

Table S1. The elemental composition of site at cube from EDX spectrum in Figure S7.

	"1" site (Fig. S7a&b.)		"2" site (Fig. S7c&d.)		"3" site (Fig. S7e&f.)	
Element	Norm. content [wt.%]	Atom. content [at.%]	Norm. content [wt.%]	Atom. content [at.%]	Norm. content [wt.%]	Atom. content [at.%]
C-K	44.67	58.20	53.26	64.05	17.83	31.23
O-K	39.29	38.43	37.84	34.17	45.47	59.79
Mg-K	2.10	1.35	1.47	0.87	-	-
Ca-K	0.70	0.27	-	-	7.11	3.73
Sn-L	13.24	1.75	7.43	0.90	29.60	5.25

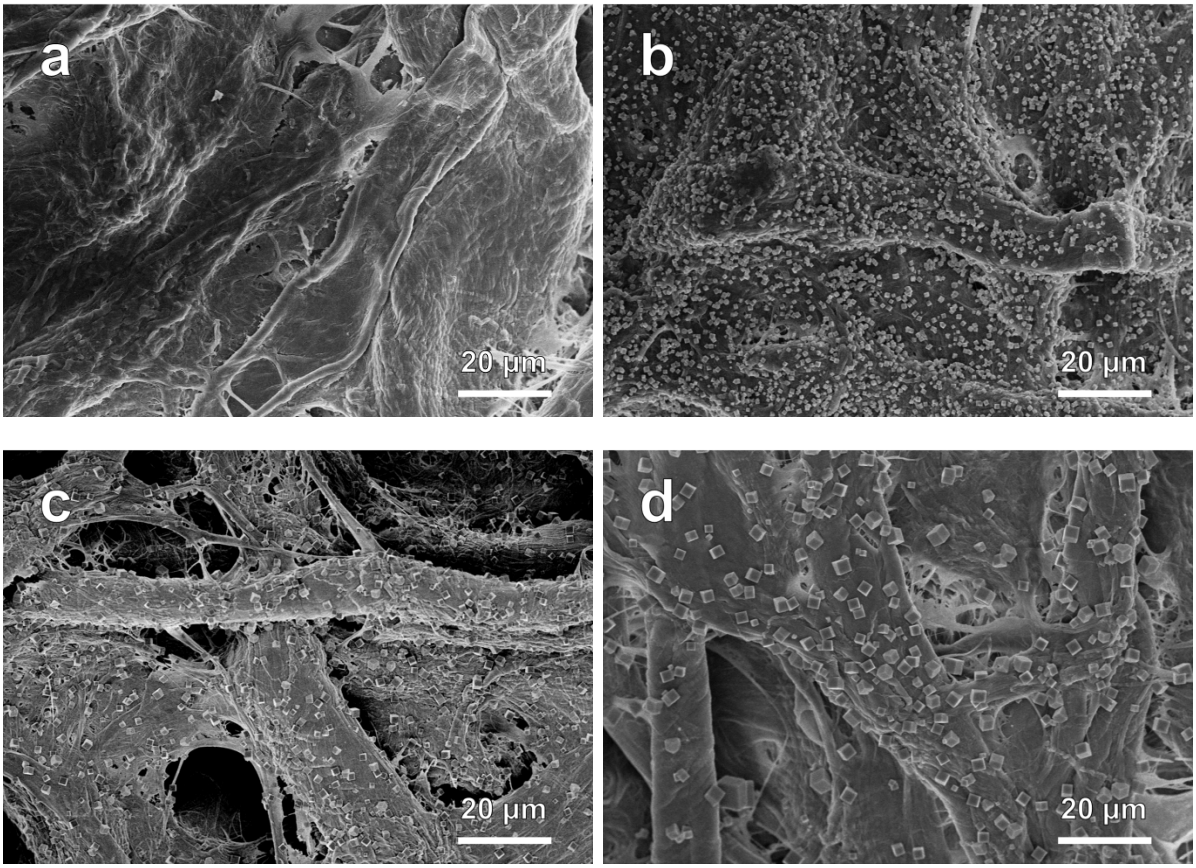

Figure S8. Representative FE-SEM images of composite paper after treating the absorbed composite paper in boiling Mg^{2+}/Ca^{2+}-containing water (300 mL) with different amounts of $NH_3 \cdot H_2O$ for 1 h: (a) 0 mL; (b) 1 mL; (c) 3 mL; and (d) 5 mL.

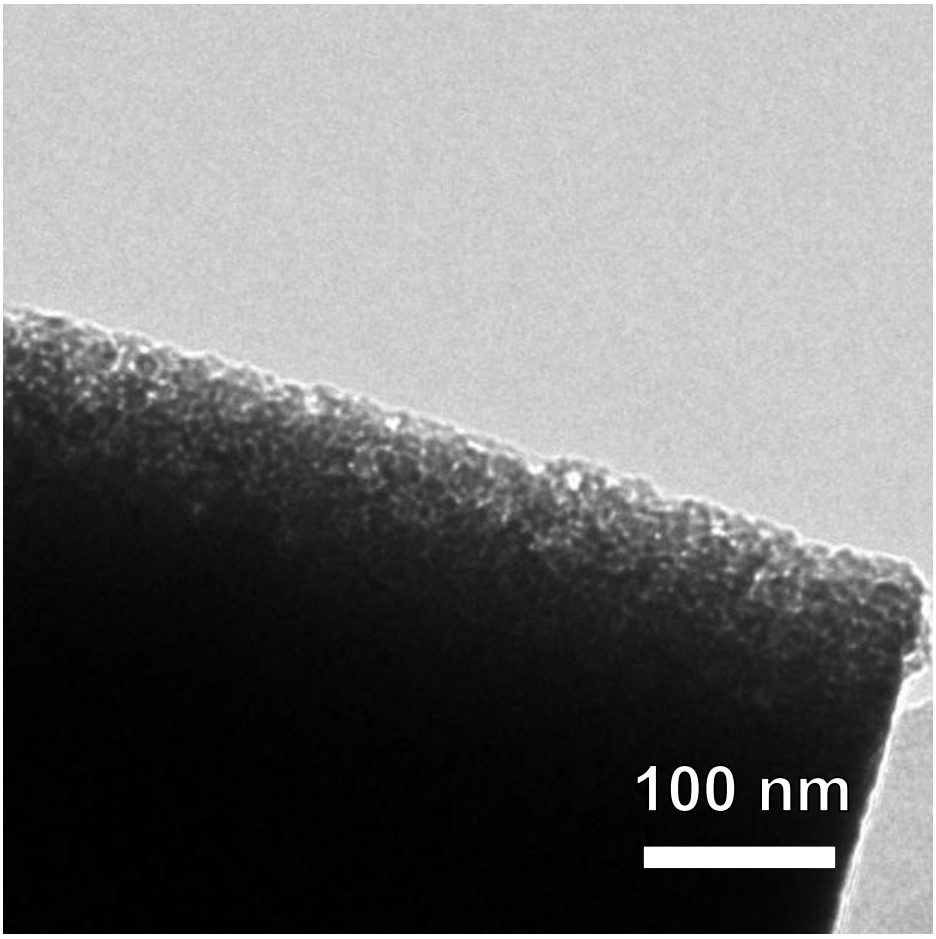

Figure S9. TEM image of the edge of MgO-CaO-SnO_x cube calcined at 600 °C for 3 h.

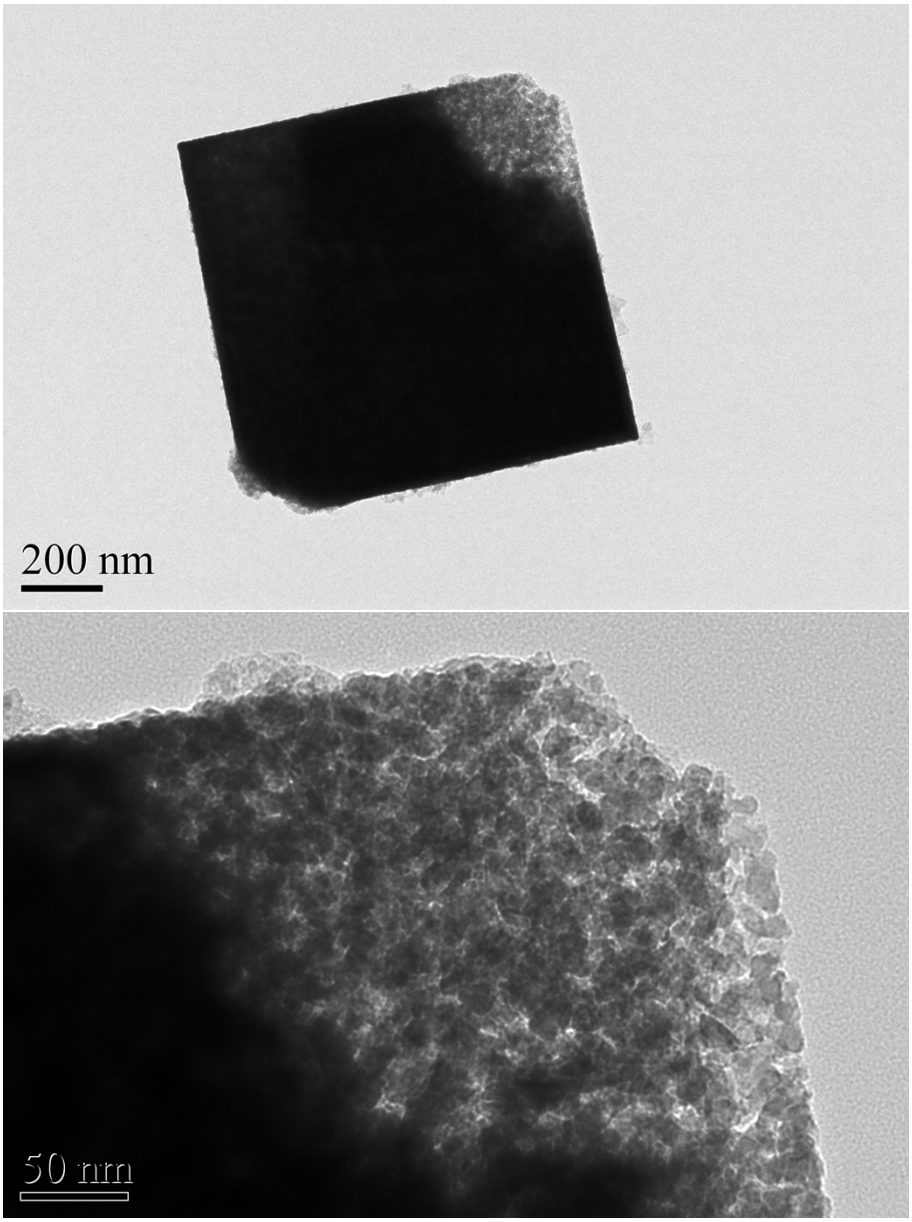

Figure S10. TEM images of a broken MgO-CaO-SnO_x cube calcined at 700 °C for 1 h.

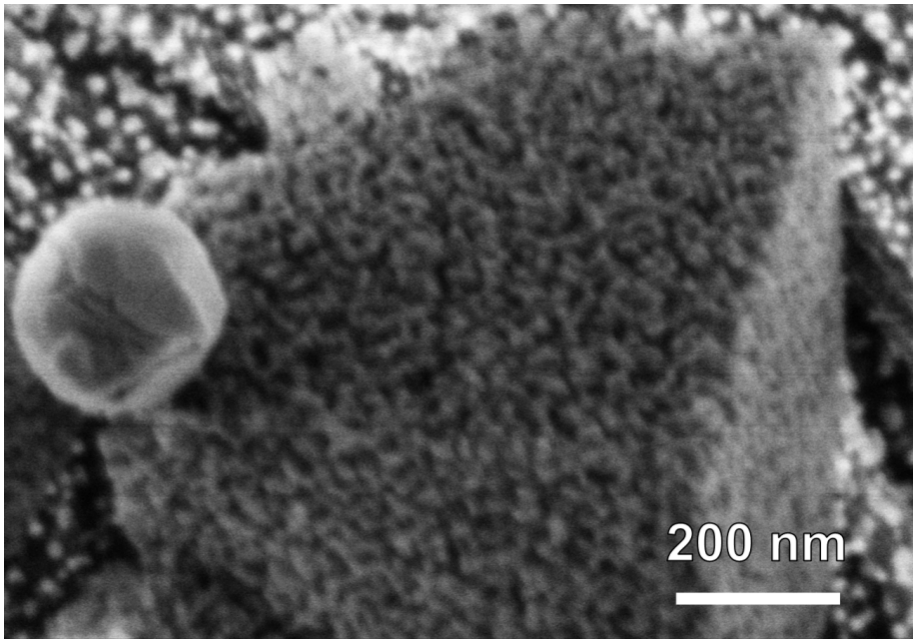

Figure S11. A magnified FE-SEM image of MgO-CaO-SnO_x-cube/carbon paper calcined at 800 °C for 1 h.

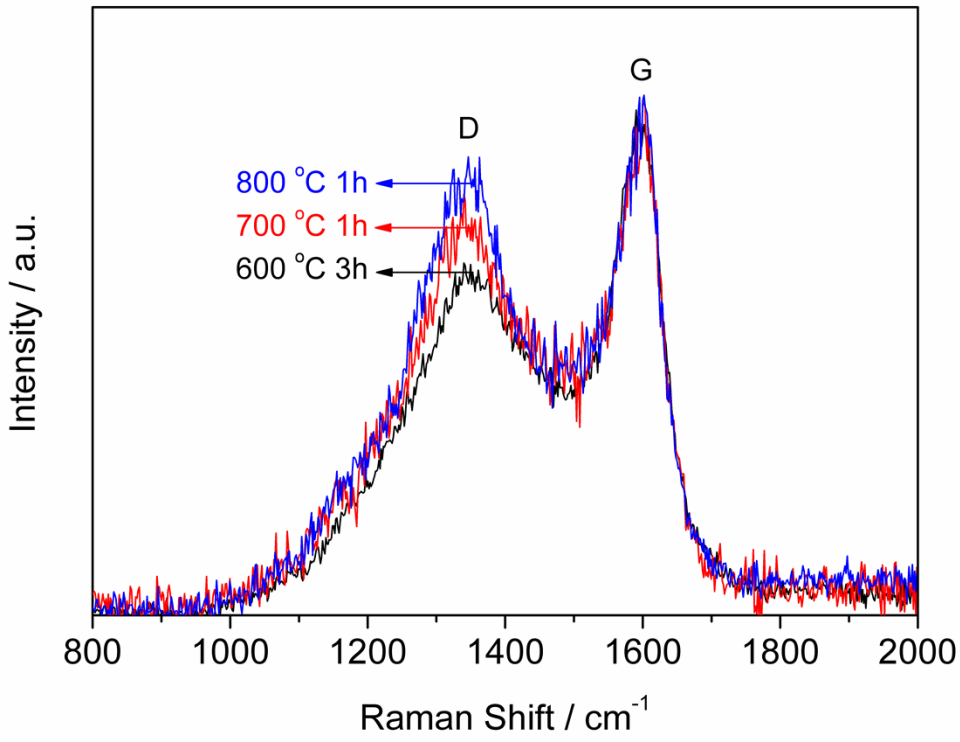

Figure S12. Raman spectra of MgO-CaO-SnO_x/carbon paper obtained at 600 °C for 3 h, 700 °C for 1 h, and 800 °C for 1 h, respectively. The Raman intensity of sample obtained at 600 °C for 3 h is multiplied by a factor of 0.22. The G band could be adjusted to coincide, and then the graphitization degree of all samples could be clearly distinguished.

The samples were also studied using Raman measurement. The results from the Raman spectra indicated that the graphitization degree decreased as the calcination temperature increased. This was different from the common understanding that the higher temperature for carbon lead to higher graphitization degree. It may be caused by the reaction between carbon and SnO_x, which resulted in formation of more disordered carbon.

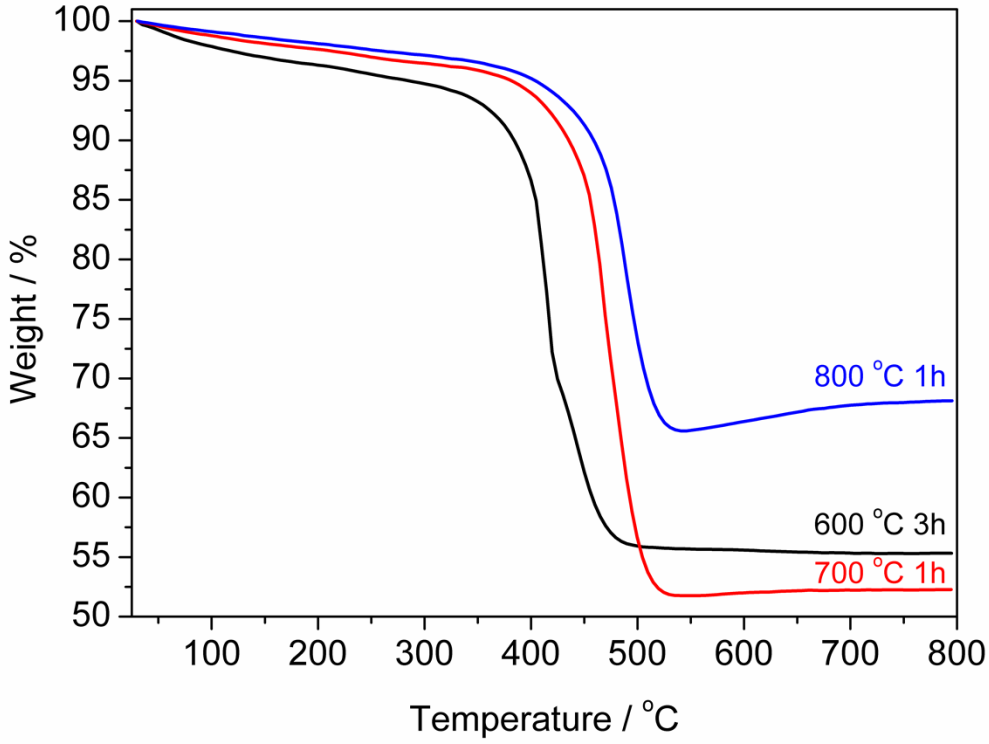

Figure S13. Thermogravimetric analysis (TGA) of MgO-CaO-SnO_x/carbon paper obtained at 600 °C for 3 h, 700 °C for 1 h, and 800 °C for 1 h, respectively.

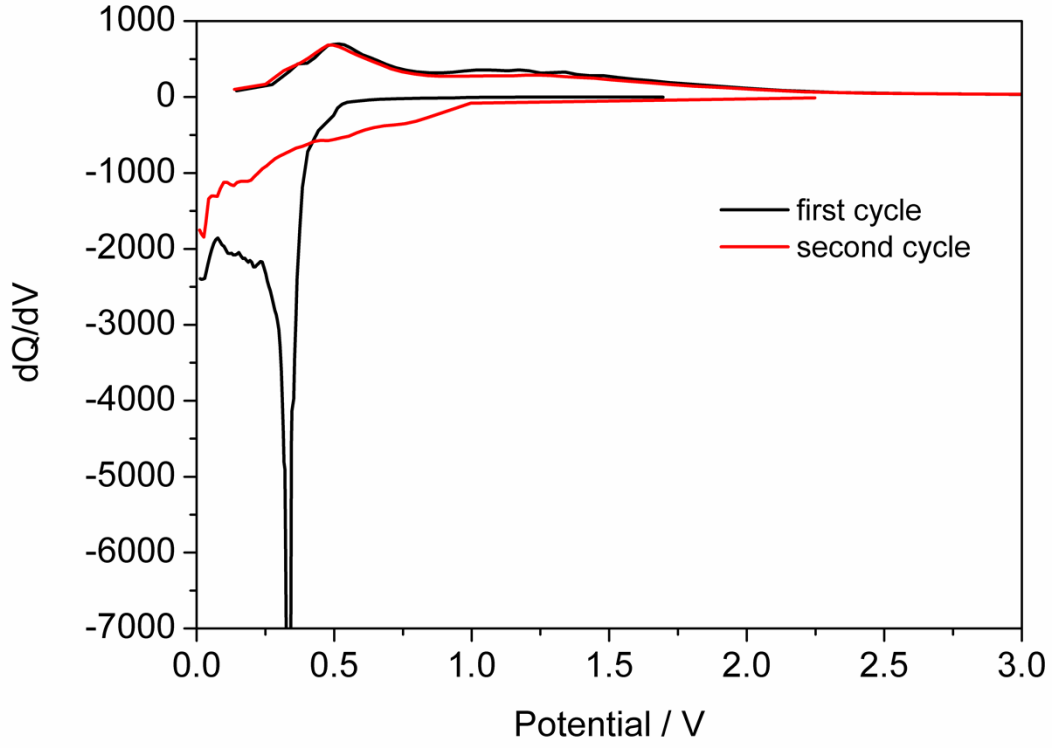

Figure S14. Corresponding differential capacity plots of the MgO-CaO-SnO_x-nanocubes/carbon paper electrode obtained at 600 °C for 3 h at 100 mA g^{-1} in the potential range of 0.01–3.0 V.

Shown in Figure S14, a cathodic peak appeared at round 0.33 V in the first cycle and disappeared in the second cycle, which could be attributed to the conversion of SnO_x to Sn and the formation of solid–electrolyte interface (SEI) layer. There was characteristic pair of cathodic and anodic peaks at round 0.15 V and 0.50 V in the both first and second cycles, which was related to reversible alloying and de-alloying processes, respectively.

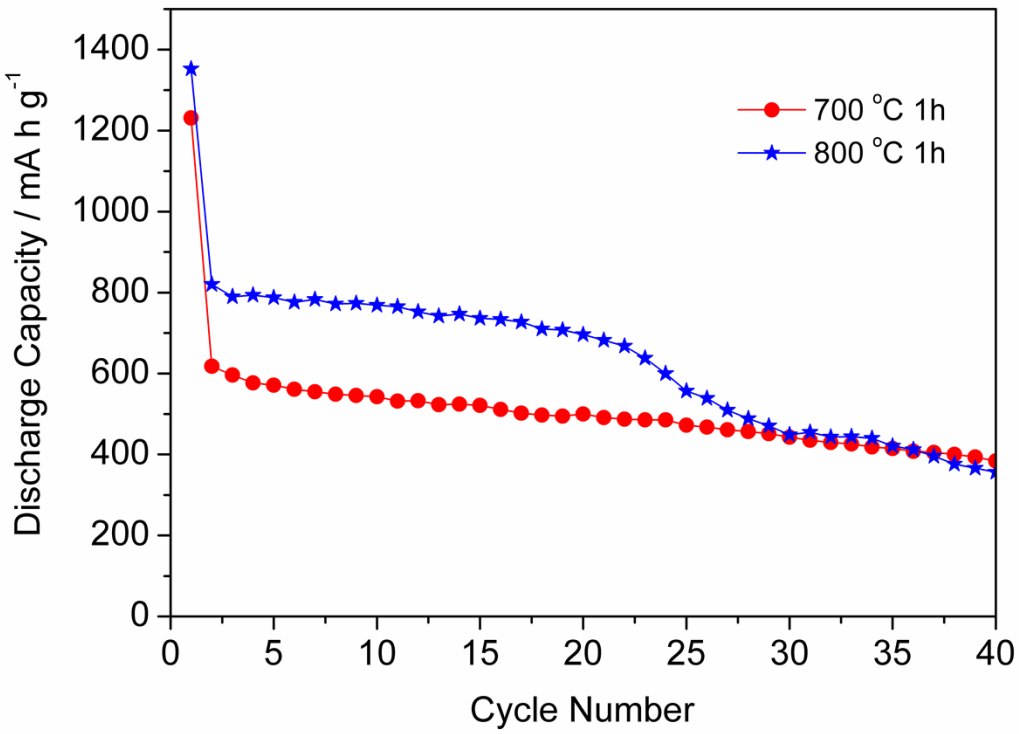

Figure S15. Cycling performance of the cells with MgO-CaO-SnO_x-nanocubes/carbon paper electrodes obtained at 700 °C for 1 h and 800 °C for 1 h at 100 mA g^{-1} in the potential range of 0.01–3.0 V.